

1 **A ratiometric sensor based on plant N-terminal degrons able to report oxygen dynamics in**
2 ***Saccharomyces cerevisiae***

3 Mikel Lavilla Puerta¹, Vinay Shukla¹, Laura Dalle Carbonare¹, Daan A. Weits¹, Pierdomenico Perata¹,
4 Francesco Licausi^{1,2*}, Beatrice Giuntoli^{1,2*}

5 ¹ Plantlab, Institute of Life Sciences, Scuola Superiore Sant'Anna, Via Guidiccioni 8/10c, 56010, Ghezzano
6 (PI), Italy

7 ²Department of Biology, University of Pisa, Via Luca Ghini 13, 56126, Pisa, Italy

8 * Senior authors

9 **Corresponding author:**

10 Francesco Licausi

11 francesco.licausi@unipi.it

12 Phone: +39050881914

13 Fax: +39050881913

14

15 **Abstract**

16 The ability to perceive oxygen levels is crucial to many organisms because it allows discerning environments
17 compatible with aerobic or anaerobic metabolism, as well as enabling rapid switch between these two
18 energy strategies. Organisms from different taxa dedicate distinct mechanisms to associate oxygen
19 fluctuations with biological responses. Following from this observation, we speculated that orthogonal
20 oxygen sensing devices can be created by transfer of essential modules from one species to another in
21 which they are not conserved. We expressed plant cysteine oxidase enzymes (PCOs) in *Saccharomyces*
22 *cerevisiae*, to confer oxygen-conditional degradability to a bioluminescent protein tagged with the Cys-
23 exposing N-degron typical of plant ERF-VII factors. Co-translation of a second luciferase protein, not
24 subjected to oxygen-dependent proteolysis, made the resulting Double Luciferase Oxygen Reporter (DLOR)
25 ratiometric. We show that DLOR acts as a proxy for oxygen dynamics in yeast cultures. Moreover, since
26 DLOR activity was enabled by the PCO sensors, we employed this device to disclose some of their
27 properties, such as the dispensability of nitric oxide for N-terminal cysteine oxidation and the individual
28 performance of Arabidopsis PCO isoforms *in vivo*. In the future, we propose the synthetic DLOR device as a
29 convenient, eukaryotic cell-based tool to easily screen substrates and inhibitors of cysteine oxidase
30 enzymes *in vivo*. Replacement of the luminescent proteins with fluorescent proteins will further turn our
31 system into a visual reporter for oxygen dynamics in living cells.

32 **Keywords:** N-end rule pathway, oxygen sensing, plant cysteine oxidase, synthetic biology, *Saccharomyces*
33 *cerevisiae*

34 Abbreviations: cPTIO, 2-(4-carboxyphenyl)-4,4,5,5-tetramethylimidazolinone-1-oxyl-3-oxide; ERF-VII,
35 ethylene response factor VII; PCO, plant cysteine oxidase; SNAP, S-nitroso-N-acetylpenicillamine,

36

37 **Introduction**

38 Numerous perception mechanisms to cope with varying oxygen levels have been identified across
39 biological kingdoms, each optimized to the ecological niche occupied and the biological process being
40 controlled. Remarkably, transcriptional regulation of low oxygen responses in eukaryotes converged
41 towards a similar solution, based on proteolytic control of transcription factors by means of oxidative
42 reactions [1]. In animal cells, the stability and activity of the transcription factor HIF-1 [2–6] is controlled by
43 proline and asparagine hydroxylation, catalysed by 2-oxoglutarate and oxygen dependent hydroxylases
44 [7,8]. The same class of enzymes is involved in controlling the half-life of sterol regulatory element binding
45 proteins (SREBPs)[9], regulators of lipid homeostasis and metal uptake in different fungal species [10].
46 These ER-tethered transcription factors are tied to hypoxia by a twofold layer of regulation. In addition to
47 direct oxidation through prolyl hydroxylases, their N-terminal fragment is endoproteolytically cleaved and
48 released into the nucleus when sterol levels drop because of insufficient oxygen availability [11,12].

49 Instead, a different oxidative reaction is dedicated to oxygen-controlled gene expression in higher plants.
50 Here, dioxygenation of amino-terminal cysteine of the group VII of the ethylene responsive factor (ERF-VII)
51 family generates a sulfinylated residue that stimulates protein degradation via the 26S proteasome [13,14].
52 In this way, the induction of hypoxia-responsive genes by ERF-VII is prevented under aerobic conditions.
53 This regulation falls within a broader and interconnected sequence of post-translational modifications,
54 defined as the N-end rule pathway [15], that dictates protein stability depending on the amino-terminal
55 amino acid [16]. According to this pathway, N-terminal residues characterised by sulfinic and carboxylic
56 moieties alike are substrates of arginine conjugation by Arg-transferases (ATE) [17]. This modification
57 generates a destabilizing domain (N-degron) that can be polyubiquitinated by single subunit E3 ligase (Ub
58 ligase N-recognin1, UBR1, in yeast) [18].

59 N-terminal Cys oxidation was initially assumed to occur spontaneously in the presence of oxygen and nitric
60 oxide [19,20], leading to the designation of proteins with such N-negrans as sensors of both gaseous
61 molecules [13,21,22]. The discovery of plant cysteine oxidases (PCOs) disclosed the possibility of enzymatic

62 control over this step of N-end ruled proteolysis [23,24] thereby shifting the attribution of oxygen sensory
63 function to these proteins. While oxygen represent a co-substrate for PCO activity, the contribution of NO
64 to this process has remained more elusive, given its dispensability in *in vitro* assays but, at the same time,
65 the stabilisation of Cys-degron proteins by limiting NO accumulation *in vivo* [19,25].

66 Here, we describe the design of a synthetic reporter for oxygen levels, named DLOR (Dual Luciferase
67 Oxygen Reporter), based on the plant-derived oxygen sensory pair ERF-VII/PCO and its characterisation in
68 *Saccharomyces cerevisiae*, as a proof of concept for its exploitation in orthogonal biological systems.

69

70 **Results**

71 ***A plant-derived reporter system expressed in yeast is autonomously controlled by oxygen***

72 We built our investigation on the established N-degron substrate RAP2.12, an ERF-VII transcription factor
73 from Arabidopsis, and the plant cysteine oxidase PCO4, shown to possess maximum activity on a RAP2.12-
74 derived peptide *in vitro* [23]. To test whether the PCO/ERF-VII couple is sufficient to constitute a *bona fide*
75 oxygen sensor for eukaryotic cells, we exploited *Saccharomyces cerevisiae* as a biological chassis to express
76 a ratiometric reporter for the Arg-Cys branch of the N-end rule pathway. Following the strategy devised by
77 Varshavsky and colleagues [15], we opted for a genetic fusion of two enzymes able to emit signals of easy
78 and orthogonal detection, which are co-translationally split into single polypeptides with independent
79 fates. We opted for a *Renilla reniformis* luciferase (Rluc) separated by means of a ubiquitin monomer from
80 the N-degron of the RAP2.12 transcription factor, in turn fused to *Photinus pyralis* luciferase (Fluc).
81 Ubiquitin ensures precise cleavage by deubiquitinating enzymes [26] leaving the N-terminal cysteine from
82 the ERF-VII motif exposed [27]. The independent fate of the two cleaved modules *in vivo* could then be
83 followed upon disruptive measurement of the two luciferase activities. We speculated that forcing
84 oxidation of the exposed Cys in an O₂-dependent manner would conditionally channel the Fluc module
85 towards N-end rule proteolysis and therefore named the chimeric construct as Cys-containing Double
86 Luciferase based Oxygen Reporter (C-DLOR) (Fig. 1a). An Ala substituted version was also designed (A-

87 DLOR), containing a C2A mutation in the RAP₂₋₂₈ peptide, which is not expected to undergo conditional
88 proteolysis (Fig. 1a).

89 Coherently with the previous report that N-terminal cysteine is not a destabilizing residue in budding yeast
90 [28], expression of C-DLOR in MaV203 cells led to a relative luciferase activity (i.e. Fluc/Rluc ratio) of around
91 1 (Fig. 1b). The output of the system was not significantly modified when cells were compelled to hypoxic
92 growth (1% O₂ v/v). Instead, concomitant expression of the *Arabidopsis thaliana* cysteine oxidase PCO4
93 significantly abated the relative luciferase activity (Fig. 1b). After immunoblotting of the yeast protein
94 extracts with a Fluc antibody, we could only observe a band compatible with the DLOR cleavage product
95 (RAP2.12₂₋₂₈-Fluc), indicating complete separation of the two luciferase modules (Supplementary Fig. 1). In
96 this way, we made sure that the variable luminescent output reflected the activity of the RAP2.12₂₋₂₈-Fluc
97 module, rather than that of an intact DLOR protein. The RAP2.12₂₋₂₈-Fluc protein abundance was strikingly
98 decreased in cells expressing PCO4 under aerobic conditions, but not under hypoxia, while Rluc was
99 unaffected by either PCO4 expression or oxygen availability (Fig. 1c and 1d). To make sure that DLOR
100 dynamics were due to post-translational events, we also measured the mRNA levels of the sensor
101 components. *Fluc* and *PCO4* transgene expression was not altered by the hypoxic treatment, whose
102 effectiveness was verified by the induction of the hypoxia responsive gene *CYC7* [29] (Supplementary Fig.
103 2a). We could therefore exclude the existence of transcriptional regulation on DLOR. Little C-DLOR residual
104 activity was observed in PCO4-containing aerobic cells, accounting for approximately 10% of the output
105 reached under hypoxia (Fig. 1b, 1e and 1f). Persistence of a fraction of reporter module protein could
106 derive from excessive DLOR production, as related to PCO4 processing capacity. It is conceivable that
107 reciprocal tuning of DLOR and PCO transcription and/or translation rates would lead to further improved
108 dynamic range of the sensor.

109 Taken together, this data showed that no native PCO-like activity is encoded by the yeast genome, in
110 agreement with the fact that no PCO-homolog could be retrieved by blast interrogation of the *S. cerevisiae*
111 proteome (Supplementary Fig. 2b). Moreover, our results demonstrated that, once introduced in yeast,
112 PCO4 retains the ability to restrain the abundance of Cys-exposing proteins in the presence of oxygen,

113 compatibly with its oxygen sensing capacity. In conclusion, it can be stated that the DLOR/PCO4 pair works
114 in an orthogonal fashion to the oxygen sensing mechanisms active in yeast to generate an oxygen-
115 dependent output.

116 ***Regulation of DLOR activity via the N-end rule pathway***

117 We next tested whether PCO4-induced DLOR proteolysis in *S. cerevisiae* is mediated by the N-end rule
118 pathway. Cys substitution with Ala entirely prevented PCO4-driven reduction of reporter output under
119 aerobic conditions (Fig. 1e), demonstrating that N-terminal Cys is required to achieve the aerobic
120 degradation of the Fluc module. Immuno-detection displayed no major changes in the Fluc protein amount
121 when A-DLOR was expressed in the presence of PCO4 in either ambient (21% O₂) or hypoxic (1% O₂)
122 atmosphere (Supplementary Fig. 3a). The superior sensitivity of the dual luciferase assay also hinted at
123 some additional oxidation-independent activity by PCO4, only achievable at low oxygen concentrations and
124 requiring an N-terminal alanine residue (Fig. 1e). Taken together, these results confirmed that PCO4 confers
125 oxygen-dependent protein instability to Fluc through the Cys N-degron pathway.

126 Consequently, we investigated whether such regulation relies on the functionality of the Arg/N-end rule
127 pathway. To this purpose, we targeted the genomic ATE1 locus, responsible for the N-terminal conjugation
128 of Arg that generates a UBR1 substrate, and replaced it with a kanamycin resistance cassette
129 (Supplementary Fig. 3b) thereby abolishing ATE1 expression (Supplementary Fig. 3c). In the mutant
130 *ate1Δ::KanMX4* strain, C-DLOR exhibited constant activity irrespectively of the expression of PCO4 (Fig. 1f):
131 thus, we concluded that PCO4 promotes Fluc degradation via the N-end rule pathway.

132 Despite conservation across the three eukaryotic kingdoms of ATE and UBR enzymes, and of the overall
133 regulation of protein stability according to the N-end rule pathway [17], N-terminal cysteine does not
134 constitute a destabilizing residue in *S. cerevisiae* [28]. It has been hypothesized that insufficient nitric oxide
135 (NO) levels did not permit Cys oxidation in the presence of oxygen, preventing the production of the N-
136 degron [19,30]. However, substantial NO accumulation in *S. cerevisiae* has lately been detected and
137 attributed to either NOS-like activity or nitrite reduction [31]. Moreover, PCO's need for NO to promote

138 ERF-VII degradation in plants is still debated [23], considering that purified PCO enzymes can catalyse
139 substrate oxidation in the absence of NO donors *in vitro* [32]. The DLOR reporter represents an ideal system
140 to address these questions, due to its specificity for PCOs. We first tested whether the supplementation of
141 a chemical NO donor (S-nitroso-N-acetylpenicillamine, SNAP) was able to reduce reporter output under
142 aerobic conditions. In the absence of PCO4, SNAP did not affect significantly C-DLOR activity (Fig. 1g). We
143 confirmed the efficacy of the treatment by measuring the expression of Copper Transporter 1 (*CTR1*), an
144 NO-induced gene [33]; *CTR1* mRNA rapidly increased upon NO stimulation, falling back to untreated levels
145 after 5 h (Supplementary Fig. 4). We therefore concluded that absence of Cys oxidase enzymes, rather than
146 low NO levels, excludes cysteine from the list of destabilizing residues in budding yeast. Additionally, in cells
147 expressing both transgenes the NO scavenger 2-4-carboxyphenyl-4,4,5,5-tetramethylimidazoline-1-oxyl-3-
148 oxide (cPTIO) did not affect PCO4-promoted DLOR instability (Fig. 1h), suggesting that PCO4 does not
149 require NO to stimulate the degradation of protein exposing an N-terminal cysteine in living *S. cerevisiae*
150 cells.

151 ***DLOR reports intracellular oxygen concentrations in growing yeast cultures***

152 The results described so far prompted us to extend the characterisation of the oxygen-dependent
153 regulation imposed by PCO4, by describing DLOR activity as a function of oxygen availability. Aerobic
154 cultures were split and incubated at different external oxygen concentrations for an equal amount of time
155 (6 h). An atmosphere containing 3% O₂ (v/v) was able to significantly elevate DLOR signal over aerobic
156 values, and the output rose steeply when oxygen levels were further diminished (Fig. 2a). The highest
157 output was reached by incubation under anoxia (100% N₂ v/v) (Fig. 2a). These data indicate that, in living
158 yeast cells, PCO4 retains full activity on the C-RAP₂₋₂₈-Fluc substrate as long as the oxygen concentration in
159 the external atmosphere remained above 5%, while it experienced quick loss of activity below 3% O₂ (v/v).

160 Next, we investigated the relationship between the luminescent output and the actual oxygen
161 concentration in the growth medium, which in turn depends on cell density, respiratory rate and
162 atmospheric oxygen availability. To this end, DLOR activity was measured in an air-equilibrated culture

163 stirred under 1% O₂ atmosphere and oxygen levels in the growth medium constantly monitored. In the first
164 hour of incubation, oxygen concentration decreased down to about 2 mg l⁻¹ (70 μM O₂, Fig. 2b) with no
165 effect on DLOR activity (Supplementary Fig. 5a): this value is equivalent with the concentration of a
166 medium equilibrated with a 5% O₂ atmosphere (V/V), the response of the sensor was in agreement with
167 previous evidence about its sensitivity (Fig. 2a). The initial decrease in dissolved oxygen was comparable in
168 the clean medium and in the one containing cells. After 130 min, instead, the medium reached a set point
169 of 0.6 mg l⁻¹ O₂, corresponding to the equilibrium with the external 1% atmosphere, while, in presence of
170 exponentially growing cells, oxygen depletion slowly carried on until near-anoxia (Supplementary Fig. 5b).
171 DLOR activation was observed at 3 h (Supplementary 5a), when oxygen concentration in the culture was
172 0.3 mg l⁻¹ (8 μM). The luminescent output maintained a linear increase over time (Fig. 2b), while, when
173 plotted as a function of O₂ concentration in the medium, it displayed an exponential behaviour
174 (Supplementary Fig. 5c). Thus, with set starting OD₆₀₀ (0.1) and external atmosphere (1% O₂), our model
175 allows to estimate the intracellular concentration of oxygen, assumed in equilibrium with the medium,
176 from DLOR output.

177 Finally, we characterised the reversibility of our synthetic system when oxygen is supplemented back.
178 Reoxygenation elicited a faster response by DLOR than hypoxia, halving the relative signal in 1 h and
179 restoring it back to aerobic levels in 4 h (Fig. 2c). Such a quick dynamics is compatible with active
180 proteolysis of the Fluc reporter through the proteasome, as compared to the slower increase of the signal
181 under hypoxia, which requires new protein synthesis.

182 ***DLOR as a tool to investigate cysteine oxidase enzyme functionality in vivo***

183 The PCO family of *A. thaliana* is comprised of five members, as identified by similarity search starting from
184 the human cysteamyl dioxygenase protein sequence (Fig. 3a). Pioneering studies by Flashman and co-
185 workers showed that Arabidopsis PCO isoforms exhibit different affinity for oxygen and ERF-VII substrates
186 *in vitro*, with PCO4 behaving as the most competent enzyme for RAP2.2 and RAP2.12 oxidation [34]. We
187 reasoned that the DLOR-based system provides an unprecedented way to extend the characterization of

188 plant PCO isoforms in terms of activity in living cells. In our hands, co-expression of the dual reporter with
189 each of the Arabidopsis isoforms revealed similar output levels for PCO1, PCO4 and PCO5 under aerobic
190 conditions, whereas DLOR activity was higher in PCO2 and PCO3 expressing cells (Fig. 3b). To investigate
191 whether these differences could be ascribed to the oxygen sensitivity of the PCO isoforms or rather to their
192 different turnover, we generated GFP-tagged versions of all five PCOs and expressed them in yeast with the
193 C-DLOR construct. First, we tested whether the GFP fusion affected the enzyme activity in air and hypoxia
194 using PCO4 as an example over the same time-course described above, obtaining comparable patterns of
195 relative luminescence (Supplementary Fig. 6a). Next, we assessed PCO protein levels, by immunoblotting,
196 along with dual luciferase activity in log-phase cultures. Six hour growth was necessary to obtain a sufficient
197 amount of cell extracts for immunoblotting from the same culture volume used before. We did not observe
198 substantial changes in the abundance of GFP-PCO1, 4 and 5 when comparing aerobic and hypoxic samples,
199 while PCO2 and 3 displayed higher degree of variability across the biological replicates (Supplementary Fig.
200 6b). Moreover, the activity of GFP-tagged versions on the DLOR response did not significantly differ from
201 that of the untagged ones (Supplementary Fig. 6c). Based on these data, we focused on PCO1, 4 and 5,
202 assuming that their turnover is not affected by hypoxia. Among these three isoforms, linear regressions
203 modelling of the hypoxic patterns indicated stronger hypoxia responsiveness for PCO4, which released the
204 inhibition significantly faster than PCO1 and PCO5 after the onset of 1% O₂ hypoxia (Fig. 3c and
205 Supplementary Table 1).

206

207 **Discussion**

208 With the introduction of the DLOR/PCO couple in budding yeast, we proved that the Arg-Cys N-end rule
209 pathway acts as a genuine oxygen perception mechanism. In plants, it has been proposed that other
210 regulatory mechanisms might be required upstream of PCO to rapidly activate ERF-VII under hypoxia.
211 Instead, the experiments reported here support the primary role of PCOs in inhibiting ERF-VII activity in an
212 oxygen dependent manner, similar to what prolyl hydroxylases do to the HIF1 transcription factor in

213 animals [3]. First, we obtained evidence that in yeast cysteine acts as a conditional degradation tag
214 exclusively when it is oxidized by PCO (Fig. 1b and 1c). Thus, spontaneous oxidation in our eukaryotic host
215 system was ruled out. Our results prove that fungal cells possess all requirements for oxygen-dependent
216 proteolysis of Cys-exposing peptides except for N-terminal Cys oxidases, providing a likely explanation to
217 the notion of Cys not being a destabilizing residue in wild type yeast. Moreover, we showed that, once
218 isolated from their original plant background, PCOs still serve as oxygen sensors. In plants, hypothetical
219 upstream regulatory mechanisms have been proposed to link PCO activity to oxygen. However,
220 conservation of such mechanisms is unlikely in yeast, where no PCO homolog is present. Additionally,
221 oxygen independent inhibition of PCO activity by iron starvation or zinc excess also cause a hypoxia-like
222 transcriptional response [35]. Considered together, these observations seem to entail that cysteine
223 oxidases act as direct switches for oxygen also in plants. The recent reports of Cys N-degron substrates, not
224 limited to the ERF-VIIs, driving plant development also favour a main role for PCOs in driving adaptation to
225 cellular oxygen availability [36–39]. Nonetheless, this does not exclude the possibility that additional
226 indirect acute hypoxia sensing mechanisms operate aside PCO in plants. For instance, energy-dependent
227 regulation of ERF-VII localisation through changes in the cellular acyl-CoA pool has been demonstrated in
228 *Arabidopsis* [40]. Moreover, it has been proposed that reactive oxygen species caused by an impaired
229 mitochondrial electron transport could regulate membrane channels and trigger secondary signalling [41].

230 The involvement of nitric oxide in the processing of Cys/N-end rule substrates is still matter of
231 investigation. An *in vitro* arginylation assay on a Cys-starting RGS4 peptide has proven sensitive to the
232 presence of NO donors [19], leading to the conclusion that Cys oxidation could be spontaneous and
233 dependent on the concomitant presence of NO. Opposite to it, other assays indicate that the oxidation and
234 arginylation of RAP2.12-derived N-termini can take place in a reaction environment completely devoid of
235 NO, when PCO and oxygen are provided [26]. In plants, NO promotes instability of some Cys-starting
236 proteins and thus has been hypothesized as a requisite for the PCO-catalyzed oxidation of N-terminal
237 cysteine *in vivo* [22,26,29]. In our *in vivo* assay, we observed that PCO4 could promote the turnover of the
238 reporter independently of NO (Fig. 1g and Supplementary Fig. 4). As we demonstrated that DLOR is able to

239 recapitulate PCO activity in a heterologous system, our data suggest that in plants nitric oxide is rather
240 likely to act in parallel to thiol oxidase enzymes to modulate the stability of Cys/N-end rule substrates.

241 The approach to generate a genetically encoded oxygen sensor is specular to the one recently attempted
242 by us for plant cells, where we exploited the animal hypoxia signalling pathway [42]. In both systems, the
243 output relies on long-lived luciferase enzymes. Their replacement with variants with fast turnover will be
244 instrumental to trigger a prompter DLOR response to oxygen dynamics. Furthermore, the same ratiometric
245 strategy adopted in the design of the sensor described here might be exploited for the design of a visual
246 reporter of oxygen. Substitution of the luciferase modules with short-lived fluorescent proteins (e.g. fast-
247 turning GFP and RFP versions) would easily turn the disruptive DLOR sensor into a dynamic reporter for
248 oxygen in live cells. Nevertheless, in its present form, DLOR can already be proposed as a suitable system
249 for the identification of inhibitors of terminal cysteine oxidases. In the same way, we envision to employ it
250 in the screening of novel substrates to expand the set of proteins subjected to the Arg-Cys branch of the N-
251 end rule pathway.

252

253 **Materials and Methods**

254 **Yeast strains**

255 The haploid *S. cerevisiae* MaV203 strain (*MAT α* ; *leu2-3,112*; *trp1-901*; *his3 Δ 200*; *ade2-101*; *cyh2^R*; *can1^R*;
256 *gal4 Δ* ; *gal80 Δ* ; *GAL1::lacZ*; *HIS3_{UASGAL1}::HIS3@LYS2*; *SPAL10::URA3*) was purchased from Thermo-Fisher
257 Scientific. *S. cerevisiae ate1 Δ ::KanMX4* strain was generated from haploid yeast (MaV203) by homologous
258 recombination following the protocol described by Gardner & Jaspersen, 2014 [43]. A synthetic
259 *ate1 Δ ::KanMX4* homology repair cassette [44] was used that contained 60 nucleotides homology arms with
260 the 5' and 3' genomic regions flanking the coding sequence of the *Saccharomyces ATE1* gene
261 (Supplementary Fig. 2b).

262 **Yeast culture**

263 *S. cerevisiae* colonies were grown at 30°C in liquid yeast synthetic medium, containing 6.7 g l⁻¹ Yeast
264 Nitrogen Base (DIFCO), 1.37 g l⁻¹ Yeast Dropout Medium (Sigma-Aldrich) and 20 g l⁻¹ glucose, plus suitable
265 supplements (0.16 M uracil, 0.8 M histidine-HCl, 0.8 M leucine and 0.32 M tryptophan when complete).
266 Overnight cultures were diluted to OD₆₀₀ 0.1 (for treatments up to 6 h long) or 0.05 (for treatments longer
267 than 6 h) in 50 mL Falcon tubes and grown at 150 rpm for the duration of the treatments at 30°C. In all
268 cases, the duration of the treatments never exceeded the time span associated to the exponential growth
269 phase. At the end of the treatments, cells were collected by centrifugation for subsequent gene expression
270 analyses, protein immunoblotting and luciferase activity assays. In case of growth on plates, media were
271 supplemented with 20 g l⁻¹ micro agar (Sigma-Aldrich).

272 **Production of yeast expression plasmids**

273 All PCR amplifications were carried out using Phusion polymerase (Thermo-Fisher Scientific). Expression
274 plasmids were propagated in Mach1 *E. coli* cells (Thermo Fisher Scientific). DLOR constructs were obtained
275 by gene synthesis by GeneArt (Thermo Fisher Scientific). The full C-DLOR cassette (RLuc-UBQ-RAP₂₋₂₈-Fluc)
276 was ligated into pENTRTM/D-TOPO[®] (Thermo Fisher Scientific). The resulting entry plasmid was exploited as
277 a template for site-directed mutagenesis of the Cys-encoding triplet (TGT) into an Ala-encoding one (GCT),
278 using DLOR_CtoAFw and DLOR_CtoARv primers (Supplementary Table 2), to obtain the A-DLOR entry
279 plasmid. Both DLOR constructs were recombined into the integrative vector pAG304GPD-ccdB (Addgene
280 plasmid #14136) with the Gateway LR Clonase II Enzyme mix (Thermo Fisher Scientific), to drive DLOR
281 expression under control of the glyceraldehyde-3-phosphate dehydrogenase (*GAP*) promoter.

282 The coding sequences of the five *PCO* (Plant Cysteine Oxidase) genes were amplified from Arabidopsis
283 cDNA, retro-transcribed by means of the Maxima First Strand cDNA Synthesis Kit (Thermo Fisher Scientific),
284 using the specific primers described in Supplementary Table S2 and cloned into pENTRTM/D-TOPO[®]. The
285 *PCO* containing entry plasmids were recombined into the pAG415GPD-ccdB vector (Addgene plasmid
286 #14146), to direct their constitutive expression under control of the *GAP* promoter. The GFP-tagged

287 versions were generated by recombination in the pAG415GPD-EGFP-ccdB destination vector (Addgene
288 plasmid #14314).

289 **Yeast transformation**

290 Yeast competent cells were produced and transformed with the FCC-LiAc method, following the protocol
291 described by Gietz, 2007 [45]. pAG304GPD-DLOR and pAG304GPD-ccdB plasmids were linearized with BstXI
292 (Thermo Fisher Scientific) prior to transformation. Colonies bearing the recombined pAG304GPD-DLOR and
293 pAG415GPD-PCO plasmids, or the empty (unrecombined) plasmids used as negative controls, were
294 selected based on auxotrophy complementation, on tryptophan- or leucine-defective plates respectively. A
295 synthetic *ate1Δ::KanMX4* sequence (Gene Art; Supplementary File 1) was amplified with primers
296 *ate1Δ::KanMX4Fw* and *ate1Δ::KanMX4Rv*. Once purified, the PCR product was directly delivered to
297 competent MaV203 bearing the pAG304GPD-DLOR and pAG415GPD-PCO constructs, according to Gietz,
298 2007 [45]. Recombinants were selected on plates containing 300 μM G418 (Sigma-Aldrich) and lacking
299 tryptophan and leucine.

300 **Low oxygen treatments**

301 Air equilibrated cultures from over-night growth were diluted to $OD_{600}=0.1$ and moved to hypoxic growth
302 conditions into a Gloveless Anaerobic chamber (COY), or returned to the original incubator in the case of
303 aerobic control cultures. The built-in gas mixing system was exploited to reach the desired oxygen
304 concentration in the internal environment of the anaerobic chamber, upon blending of nitrogen gas with
305 atmospheric air. Constant temperature of 30°C and shaking of 150 rpm were maintained along all
306 treatments, which were protracted for the time specified in each experiment. Repeated samplings from the
307 same culture were carried out in time-course experiments.

308 **Chemical treatments**

309 300 μM SNAP (S-nitroso-N-acetylpenicillamine, Sigma-Aldrich) or 200 μM cPTiO (2-4-carboxyphenyl-4,4,5,5-
310 tetramethylimidazoline-1-oxyl-3-oxide, Sigma-Aldrich) in 0.1% DMSO (v/v) were applied to growing yeast

311 cultures at $OD_{600}=0.1$. Mock-treated cultures were supplemented with 0.1% DMSO (v/v). Treatments were
312 protracted for the specified time.

313 **Measurement of relative luciferase activity**

314 Luciferase activity was quantified from 50 μ L yeast culture using the Dual-Luciferase[®] Reporter (DLR[™])
315 Assay System (Promega). Cells grown as described in the section “Yeast culture” were recovered by
316 centrifugation and pellets were lysed in 50 μ L 1x Passive Lysis Buffer. Luciferase activities measured
317 according to the manufacturer’s protocols, using a Lumat LB 9507 Tube Luminometer (Berthold). Data were
318 expressed as Fluc/Rluc signal ratio (“relative Fluc activity”).

319 **Immunoblotting**

320 Total *S. cerevisiae* proteins were extracted following von der Haar et al. [46]. In brief, cells were incubated
321 in 100 mM NaOH, 50 mM EDTA and 2% SDS at 90°C for 10 min before adding acetic acid to a final
322 concentration of 100 mM. Samples were incubated as described above and spun at top speed to remove
323 cell debris. Soluble protein extract were denatured, loaded on polyacrylamide gels (NuPage Bis-Tris Gels,
324 Thermo Fisher Scientific) and separated via SDS-PAGE. Proteins were transferred on a polyvinylidene
325 difluoride membrane (Bio-Rad) using the TransBlot[®] Turbo transfer system (Bio-Rad). To obtain a positive
326 control for the DLOR modules, a wheat germ extract expressing the construct was loaded along with the
327 yeast cell lysates. To this end, the construct was cloned in the pF3A WG (BYDV) Flexi[®] Vector (Promega) and
328 the resulting expression vector was transcribed and translated in vitro with the TnT[®] Coupled Wheat Germ
329 Extract Systems (Promega), following the manufacturer’s recommendations.

330 For the immunodetection, a polyclonal anti-Fluc (G7451, Promega, used at 1000 fold dilution), a
331 monoclonal anti-Rluc (MAB4410, Millipore, used at 1000 fold dilution) and a monoclonal anti-GFP antibody
332 (11814460001, Roche, used at 2000 fold dilution) were diluted in 4% skim milk solution in PBST to detect
333 firefly luciferase, renilla luciferase and GFP, respectively. Secondary anti-Mouse IgG HRP-conjugated
334 (~~A8919, Sigma-Aldrich, 1:1000~~) was used to detect renilla luciferase and GFP, anti-Rabbit IgG HRP-
335 conjugated (AS09 602, Agrisera, 1:10000) for firefly luciferase. The detection was carried out by means of

336 the SuperSignal™ West Dura (Thermo Fisher Scientific). Protein loading on the gels was evaluated by
337 membrane staining with 0.1% amido black 10-B, in 45% methanol and 10% acetic acid, followed by
338 decoloration in 90% methanol and 2% acetic acid. Signal detection took place in a ChemiDoc™ MP Imaging
339 System (Bio-Rad). Blots are representative images following the analysis of four independent clones of each
340 genotype.

341 **Gene expression analyses**

342 Yeast total RNA isolation was carried out as described by Schmitt et al. [47] with minor modifications. *S.*
343 *cerevisiae* cells were resuspended in 50 mM sodium acetate, 10 mM EDTA and 1% SDS. An equal amount of
344 phenol was added to the cell suspension. Samples were vortexed and incubated at 65°C for 4 min first, and
345 then at -20°C for 15 minutes, before centrifugation at top speed for 2 min. The aqueous phase was
346 recovered and subjected to sequential phenol: chloroform: isoamyl alcohol (25:24:1) and chloroform phase
347 extraction. Finally, nucleic acids were precipitated by centrifugation from the aqueous phase, using 2
348 volumes of ice-cold absolute ethanol supplemented with sodium acetate at a final concentration of 300
349 mM. Pellets were resuspended in RNase-free water. RNA concentration was measured using a µdropp
350 plate reader (Thermo Fisher Scientific) and its quality was checked by electrophoresis in 1% agarose gels.
351 Total RNA was then processed with Maxima cDNA synthesis kit (Thermo Fisher Scientific) using 1 µg total
352 RNA, according to the manufacturer's protocol. Gene expression levels were assessed by Real-Time qPCR,
353 using the PowerUp SYBR® Green Master Mix (Thermo Fisher Scientific) and a 7300 Real Time PCR System
354 (Applied Biosystems). Gene specific primers and their sequences are listed in Supplementary Table 2.
355 Relative gene expression was calculated according to the $\Delta\Delta C_t$ method [48], using *Actin 1* as the
356 housekeeping gene.

357 **Oxygen concentration measurements**

358 Oxygen levels were assessed live in the sterile yeast growth medium and in the medium containing a
359 growing yeast suspension, in separate experiments. Oxygen concentration was measured with a
360 phosphorescent sensor (Firesting O₂ Optical Oxygen Meter, Pyroscience). An oxygen sensing spot was

361 attached to the inner surface of the 50 ml tube used, in contact with the growing yeast culture or with the
362 clean medium. A SPADBAS adapter held the contactless sensor to the outside of the tube. Record of the
363 inner temperature was kept in a separate tube. Data was recorded using the Oxygen Logger software.

364 **Statistical analysis**

365 Cultures were started from five independent yeast colonies for each experimental thesis, unless differently
366 stated. Analyses were carried out using GraphPad Prism version 6.01 for Windows (GraphPad Software, La
367 Jolla California USA, www.graphpad.com). Statistical significance of mean differences was assessed by two-
368 way ANOVA on repeated measurements, followed by the Holm-Sidak multiple comparison test. To evaluate
369 the effect of SNAP and cPTIO on DLOR activity over time, an ANOVA on repeated measurements was
370 carried out. Box plots represent median (line) and interquartile range (IQR), whiskers span from minimum
371 to maximum values.

372

373 **Supplementary Materials**

374 Supplementary Fig. 1. Uncropped immunodetection of RAP-Fluc in DLOR cell lysates.

375 Supplementary Fig. 2. Transcription of the DLOR reporter under hypoxia and yeast proteome survey for
376 PCO homologs.

377 Supplementary Fig. 3. Regulation of DLOR according to the Arg N-end rule.

378 Supplementary Fig. 4. DLOR responses upon cell treatment with an NO donor.

379 Supplementary Fig. 5. DLOR activity under a time course of hypoxia.

380 Supplementary Table 1. Hypoxia sensitivity of Arabidopsis PCOs expressed in *S. cerevisiae* cells.

381 Supplementary Table 2. List of oligonucleotides used in this study.

382

383

384 **Acknowledgments**

385 We are grateful to Alvaro Galli and Arianna Tavanti for discussion and advices about yeast growth and
386 genetic manipulation.

387 **Funding**

388 This study was financially supported by the Scuola Superiore Sant'Anna and the University of Pisa.

389 **Author contributions**

390 M.L.P., B.G. and F.L. designed the experiments. M.L.P., V.S., L.D.C., D.A.W. and B.G. performed the
391 experiments. P.P. secured funding and provided advice about experimental strategies. B.G. and F.L. wrote
392 the manuscript and supervised the project.

393 **Competing interests**

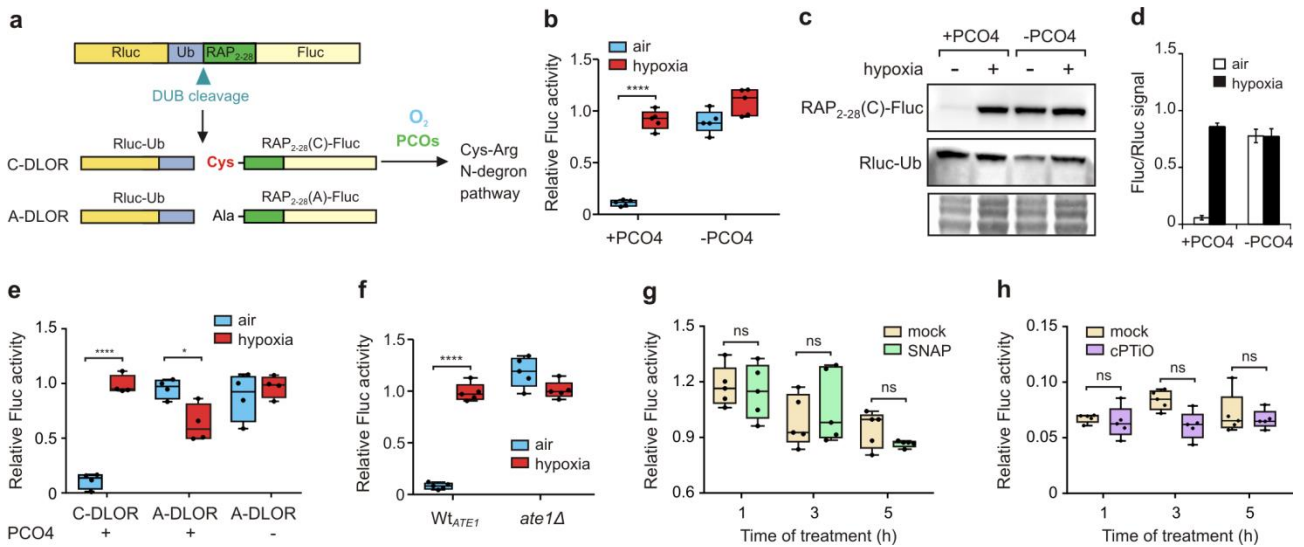
394 All authors declare the absence of any conflict of interest and any awarded or filed patents pertaining to
395 the results presented in the paper.

396 **Data and materials availability**

397 Plasmids for yeast transformation were purchased at the Addgene repository, upon signature of the due
398 MTA documents.

399

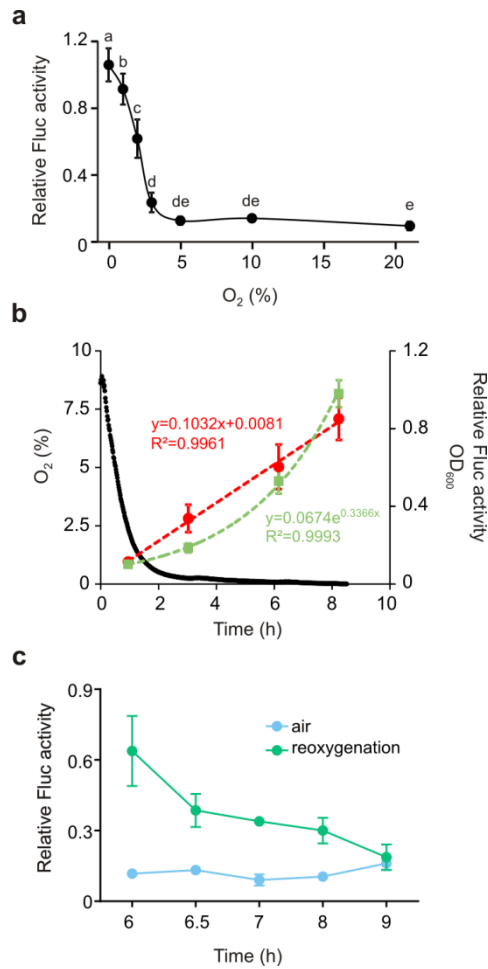
400 **Figures**



401

402 **Fig. 1 The ratiometric construct DLOR reports oxygen presence in *S. cerevisiae* when co-expressed with N-**
 403 **terminal cysteine oxidase enzyme. (a)** Design and mechanism of action of a luciferase-based oxygen
 404 reporter for yeast. **(b)** Relative Fluc activity (Fluc/Rluc ratio) in yeast cultures expressing C-DLOR along with
 405 the PCO4 enzyme (+PCO4) or alone (-PCO4), in hypoxia (1% O₂, 6 h) versus control conditions (21% O₂, 6 h).
 406 **(c)** Immunoblotting of RAP(C)-Fluc and Rluc-Ub abundance in the same cultures. A protein loading control is
 407 included. **(d)** Ratio of Fluc and Rluc protein band intensity from biological replicates shown in the
 408 immunoblots from Fig. 1c and Supplementary Fig. 1 (n=3). **(e)** Relative Fluc activity in yeast cultures (n=4)
 409 expressing PCO4 and either C-DLOR or A-DLOR under aerobic or hypoxic conditions. **(f)** Relative Fluc activity
 410 in wild-type or *ATE1* knock out mutant yeast expressing PCO4 and C-DLOR under aerobic or hypoxic
 411 conditions. All statistical comparisons shown between mean values indicate the level of significance after
 412 Two-way ANOVA on repeated measures and Holm-Sidak test. ****, $P < 0.0001$; *, $0.01 \leq P < 0.05$; ns, $P > 0.05$.
 413 **(g)** DLOR response in yeast cells treated with 300 μM SNAP or 1% DMSO (v/v; mock), in the absence of
 414 PCO4. **(h)** Effect of 200 μM cPTiO or 1% DMSO (v/v, mock) on DLOR activity in yeast cells expressing PCO4.
 415 Mean values were compared by paired t-test at each time point; ns, non-significant difference.

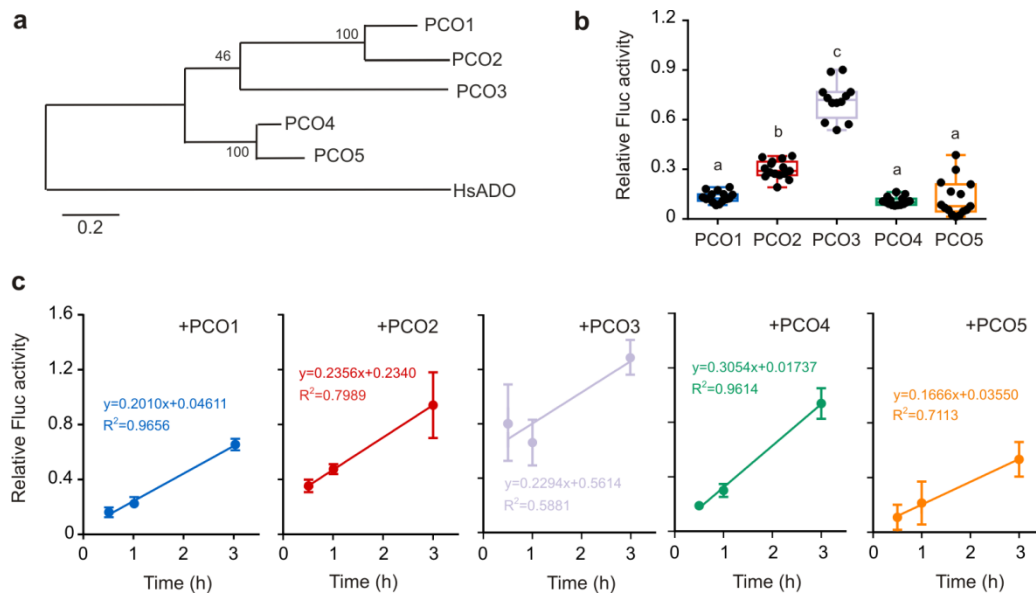
416



417

418 **Fig. 2 DLOR responds dynamically to oxygen in the presence of PCO4.** (a) DLOR activity (Fluc/Rluc ratio) in
 419 cells incubated for 6 h under different atmospheric oxygen levels (21%, 10%, 5%, 3%, 2%, 1%, or 0% O₂ v/v).
 420 Data are mean ± S.D. (n=5). Distinct letters indicate statistically significant difference among mean values,
 421 as assessed by one-way ANOVA followed by Holm-Sidak post-hoc test (P<0.05). (b) Oxygen levels (black, mg
 422 l⁻¹), relative Fluc activity (red, Fluc/Rluc) and culture density (green, OD₆₀₀) over 6 h growth under a 1% O₂
 423 atmosphere. Data for DLOR activity and cell density are mean ± S.D. (n=5). Best fit regression curves are
 424 reported (dashed lines) along with their equations. Continuous oxygen measurement in the growth
 425 medium of one culture is shown at one minute intervals. (c) DLOR activity in yeast culture shifted back to
 426 21% O₂ after 6 h hypoxic incubation (1% O₂) (green line). Cell permanently maintained in aerobic conditions
 427 are shown as a control (cyan line). Data for DLOR activity and cell density are mean ± S.D. (n=5).

428



429

430 **Fig. 3 Arabidopsis PCO isoforms impact on DLOR stability differently.** (a) Phylogenetic relatedness of the
 431 five PCO family members from Arabidopsis. A distantly related human cysteamyl dioxygenase (ADO) was
 432 included as the root. (b) Aerobic DLOR activity (Fluc/Rluc ratio) in *S. cerevisiae* cells expressing each one of
 433 the five PCO from Arabidopsis. Letters indicate the statistical significance of the differences among mean
 434 values (n=15), as assessed by one-way ANOVA followed by Holm-Sidak post-hoc test (P<0.05). (c) C-DLOR
 435 response to oxygen upon co-expression of different Arabidopsis PCOs. Data are mean ± S.D. Best fit values
 436 for linear regressions (95% C.I.) are provided.

437

438 References

- 439 [1] J.T. van Dongen, F. Licausi, Oxygen Sensing and Signaling, *Annu. Rev. Plant Biol.* (2015).
 440 doi:10.1146/annurev-arplant-043014-114813.
- 441 [2] N. Masson, C. Willam, P.H. Maxwell, C.W. Pugh, P.J. Ratcliffe, Independent function of two
 442 destruction domains in hypoxia-inducible factor-?? chains activated by prolyl hydroxylation, *EMBO J.*
 443 (2001). doi:10.1093/emboj/20.18.5197.
- 444 [3] P. Jaakkola, D.R. Mole, Y.-M. Tian, M.I. Wilson, J. Gielbert, S.J. Gaskell, A. v. Kriegsheim, H.F.
 445 Hebestreit, M. Mukherji, C.J. Schofield, P.H. Maxwell, C.W. Pugh, P.J. Ratcliffe, Targeting of HIF-alpha

- 446 to the von Hippel-Lindau Ubiquitylation Complex by O₂-Regulated Prolyl Hydroxylation, *Science* (80-
447 .). 292 (2001) 468–472. doi:10.1126/science.1059796.
- 448 [4] G.L. Wang, B.H. Jiang, E.A. Rue, G.L. Semenza, Hypoxia-inducible factor 1 is a basic-helix-loop-helix-
449 PAS heterodimer regulated by cellular O₂ tension., *Proc. Natl. Acad. Sci.* 92 (1995) 5510–5514.
450 doi:10.1073/pnas.92.12.5510.
- 451 [5] G.L. Semenza, G.L. Wang, A nuclear factor induced by hypoxia via de novo protein synthesis binds to
452 the human erythropoietin gene enhancer at a site required for transcriptional activation., *Mol. Cell.*
453 *Biol.* (1992). doi:10.1128/MCB.12.12.5447.
- 454 [6] A.C.R. Epstein, J.M. Gleadle, L.A. McNeill, K.S. Hewitson, J. O'Rourke, D.R. Mole, M. Mukherji, E.
455 Metzen, M.I. Wilson, A. Dhanda, Y.M. Tian, N. Masson, D.L. Hamilton, P. Jaakkola, R. Barstead, J.
456 Hodgkin, P.H. Maxwell, C.W. Pugh, C.J. Schofield, P.J. Ratcliffe, C. elegans EGL-9 and mammalian
457 homologs define a family of dioxygenases that regulate HIF by prolyl hydroxylation, *Cell.* 107 (2001)
458 43–54. doi:10.1016/S0092-8674(01)00507-4.
- 459 [7] D. Lando, D.J. Peet, J.J. Gorman, D.A. Whelan, M.L. Whitelaw, R.K. Bruick, FIH-1 is an asparaginyl
460 hydroxylase enzyme that regulates the transcriptional activity of hypoxia-inducible factor, *Genes*
461 *Dev.* 16 (2002) 1466–1471. doi:10.1101/gad.991402.
- 462 [8] R.J. Appelhoff, Y.M. Tian, R.R. Raval, H. Turley, A.L. Harris, C.W. Pugh, P.J. Ratcliffe, J.M. Gleadle,
463 Differential function of the prolyl hydroxylases PHD1, PHD2, and PHD3 in the regulation of hypoxia-
464 inducible factor, *J. Biol. Chem.* 279 (2004) 38458–38465. doi:10.1074/jbc.M406026200.
- 465 [9] C.Y.S. Lee, T.L. Yeh, B.T. Hughes, P.J. Espenshade, Regulation of the Sre1 hypoxic transcription factor
466 by oxygen-dependent control of DNA binding, *Mol. Cell.* (2011). doi:10.1016/j.molcel.2011.08.031.
- 467 [10] N. Grahl, K.M. Shepardson, D. Chung, R.A. Cramer, Hypoxia and fungal pathogenesis: To air or not to
468 air?, *Eukaryot. Cell.* (2012). doi:10.1128/EC.00031-12.
- 469 [11] C.M. Bien, P.J. Espenshade, Sterol regulatory element binding proteins in fungi: Hypoxic

- 470 transcription factors linked to pathogenesis, *Eukaryot. Cell.* (2010). doi:10.1128/EC.00358-09.
- 471 [12] A.L. Hughes, B.L. Todd, P.J. Espenshade, SREBP pathway responds to sterols and functions as an
472 oxygen sensor in fission yeast, *Cell.* (2005). doi:10.1016/j.cell.2005.01.012.
- 473 [13] F. Licausi, M. Kosmacz, D.A. Weits, B. Giuntoli, F.M. Giorgi, L.A.C.J. Voesenek, P. Perata, J.T. Van
474 Dongen, Oxygen sensing in plants is mediated by an N-end rule pathway for protein destabilization,
475 *Nature.* (2011). doi:10.1038/nature10536.
- 476 [14] D.J. Gibbs, S.C. Lee, N. Md Isa, S. Gramuglia, T. Fukao, G.W. Bassel, C.S. Correia, F. Corbineau, F.L.
477 Theodoulou, J. Bailey-Serres, M.J. Holdsworth, Homeostatic response to hypoxia is regulated by the
478 N-end rule pathway in plants, *Nature.* (2011). doi:10.1038/nature10534.
- 479 [15] A. Bachmair, D. Finley, A. Varshavsky, In vivo half-life of a protein is a function of its amino-terminal
480 residue, *Science* (80-.). (1986). doi:10.1126/science.3018930.
- 481 [16] A. Varshavsky, The N-end rule pathway and regulation by proteolysis., *Protein Sci.* (2011).
482 doi:10.1002/pro.666.
- 483 [17] T. Tasaki, S.M. Sriram, K.S. Park, Y.T. Kwon, The N-end rule pathway., *Annu. Rev. Biochem.* 81 (2012)
484 261–89. doi:10.1146/annurev-biochem-051710-093308.
- 485 [18] Z. Xia, A. Webster, F. Du, K. Piatkov, M. Ghislain, A. Varshavsky, Substrate-binding sites of UBR1, the
486 ubiquitin ligase of the N-end rule pathway, *J. Biol. Chem.* (2008). doi:10.1074/jbc.M802583200.
- 487 [19] R.G. Hu, J. Sheng, X. Qi, Z. Xu, T.T. Takahashi, A. Varshavsky, The N-end rule pathway as a nitric oxide
488 sensor controlling the levels of multiple regulators, *Nature.* (2005). doi:10.1038/nature04027.
- 489 [20] M.J. Lee, T. Tasaki, K. Moroi, J.Y. An, S. Kimura, I. V. Davydov, Y.T. Kwon, RGS4 and RGS5 are in vivo
490 substrates of the N-end rule pathway, *Proc. Natl. Acad. Sci.* (2005). doi:10.1073/pnas.0507533102.
- 491 [21] D.J. Gibbs, N. Mdlsa, M. Movahedi, J. Lozano-Juste, G.M. Mendiondo, S. Berckhan, N. Marín-
492 delaRosa, J. VicenteConde, C. SousaCorreia, S.P. Pearce, G.W. Bassel, B. Hamali, P. Talloji, D.F.A.

- 493 Tomé, A. Coego, J. Beynon, D. Alabadí, A. Bachmair, J. León, J.E. Gray, F.L. Theodoulou, M.J.
494 Holdsworth, Nitric Oxide Sensing in Plants Is Mediated by Proteolytic Control of Group VII ERF
495 Transcription Factors, *Mol. Cell.* (2014). doi:10.1016/j.molcel.2013.12.020.
- 496 [22] J. Vicente, G.M. Mendiondo, M. Movahedi, M. Peirats-Llobet, Y. ting Juan, Y. yen Shen, C. Dambire,
497 K. Smart, P.L. Rodriguez, Y. yung Charng, J.E. Gray, M.J. Holdsworth, The Cys-Arg/N-End Rule
498 Pathway Is a General Sensor of Abiotic Stress in Flowering Plants, *Curr. Biol.* 27 (2017) 3183–
499 3190.e4. doi:10.1016/j.cub.2017.09.006.
- 500 [23] M.D. White, M. Klecker, R.J. Hopkinson, D.A. Weits, C. Mueller, C. Naumann, R. O’Neill, J. Wickens, J.
501 Yang, J.C. Brooks-Bartlett, E.F. Garman, T.N. Grossmann, N. Dissmeyer, E. Flashman, Plant cysteine
502 oxidases are dioxygenases that directly enable arginyl transferase-catalysed arginylation of N-end
503 rule targets, *Nat. Commun.* 8 (2017). doi:10.1038/ncomms14690.
- 504 [24] D.A. Weits, B. Giuntoli, M. Kosmacz, S. Parlanti, H.M. Hubberten, H. Riegler, R. Hoefgen, P. Perata,
505 J.T. Van Dongen, F. Licausi, Plant cysteine oxidases control the oxygen-dependent branch of the N-
506 end-rule pathway, *Nat. Commun.* (2014). doi:10.1038/ncomms4425.
- 507 [25] D.J. Gibbs, J. Bacardit, A. Bachmair, M.J. Holdsworth, The eukaryotic N-end rule pathway: conserved
508 mechanisms and diverse functions., *Trends Cell Biol.* 24 (2014) 603–11.
509 doi:10.1016/j.tcb.2014.05.001.
- 510 [26] C.P. Grou, M.P. Pinto, A. V. Mendes, P. Domingues, J.E. Azevedo, The de novo synthesis of ubiquitin:
511 Identification of deubiquitinases acting on ubiquitin precursors, *Sci. Rep.* (2015).
512 doi:10.1038/srep12836.
- 513 [27] J. Bailey-Serres, T. Fukao, D.J. Gibbs, M.J. Holdsworth, S.C. Lee, F. Licausi, P. Perata, L. a C.J.
514 Voisenek, J.T. van Dongen, Making sense of low oxygen sensing, *Trends Plant Sci.* 17 (2012) 129–
515 138. doi:10.1016/j.tplants.2011.12.004.
- 516 [28] E. Graciet, F. Mesiti, F. Wellmer, Structure and evolutionary conservation of the plant N-end rule

- 517 pathway, *Plant J.* (2010). doi:10.1111/j.1365-313X.2009.04099.x.
- 518 [29] K.E. Kwast, P. V Burke, B.T. Staahl, R.O. Poyton, Oxygen sensing in yeast: evidence for the
519 involvement of the respiratory chain in regulating the transcription of a subset of hypoxic genes.,
520 *Proc. Natl. Acad. Sci. U. S. A.* (1999). doi:10.1073/PNAS.96.10.5446.
- 521 [30] R.G. Hu, C.S. Brower, H. Wang, I. V. Davydov, J. Sheng, J. Zhou, T.K. Yong, A. Varshavsky,
522 Arginyltransferase, its specificity, putative substrates, bidirectional promoter, and splicing-derived
523 isoforms, *J. Biol. Chem.* (2006). doi:10.1074/jbc.M604355200.
- 524 [31] R.I. Astuti, R. Nasuno, H. Takagi, Nitric Oxide Signalling in Yeast, in: *Adv. Microb. Physiol.*, 2018.
525 doi:10.1016/bs.ampbs.2018.01.003.
- 526 [32] M.D. White, J.J.A.G. Kamps, S. East, L.J. Taylor Kearney, E. Flashman, The plant cysteine oxidases
527 from *Arabidopsis thaliana* are kinetically tailored to act as oxygen sensors., *J. Biol. Chem.* 293 (2018)
528 11786–11795. doi:10.1074/jbc.RA118.003496.
- 529 [33] R. Nasuno, M. Aitoku, Y. Manago, A. Nishimura, Y. Sasano, H. Takagi, Nitric oxide-mediated
530 antioxidative mechanism in yeast through the activation of the transcription factor Mac1, *PLoS One.*
531 (2014). doi:10.1371/journal.pone.0113788.
- 532 [34] M.D. White, J.J.A.G. Kamps, S. East, L.J. Taylor Kearney, E. Flashman, The plant cysteine oxidases
533 from *Arabidopsis thaliana* are kinetically tailored to act as oxygen sensors, *J. Biol. Chem.* (2018).
534 doi:10.1074/jbc.RA118.003496.
- 535 [35] L. Dalle Carbonare, M. White, V. Shukla, A. Francini, P. Perata, E. Flashman, L. Sebastiani, F. Licausi,
536 Zinc excess induces a hypoxia-like response by inhibiting cysteine oxidases in poplar roots, *Plant*
537 *Physiol.* (2019) pp.01458.2018. doi:10.1104/pp.18.01458.
- 538 [36] V. Shukla, L. Lombardi, S. Iacopino, A. Pencik, O. Novak, P. Perata, B. Giuntoli, F. Licausi, Endogenous
539 Hypoxia in Lateral Root Primordia Controls Root Architecture by Antagonizing Auxin Signaling in
540 *Arabidopsis*, *Mol. Plant.* (2019). doi:10.1016/j.molp.2019.01.007.

- 541 [37] M. Abbas, S. Berckhan, D.J. Rooney, D.J. Gibbs, J. Vicente Conde, C. Sousa Correia, G.W. Bassel, N.
542 Marín-De La Rosa, J. León, D. Alabadí, M.A. Blázquez, M.J. Holdsworth, Oxygen sensing coordinates
543 photomorphogenesis to facilitate seedling survival, *Curr. Biol.* 25 (2015) 1483–1488.
544 doi:10.1016/j.cub.2015.03.060.
- 545 [38] D.J. Gibbs, H.M. Tedds, A.M. Labandera, M. Bailey, M.D. White, S. Hartman, C. Sprigg, S.L. Mogg, R.
546 Osborne, C. Dambire, T. Boeckx, Z. Paling, L.A.C.J. Voeselek, E. Flashman, M.J. Holdsworth, Oxygen-
547 dependent proteolysis regulates the stability of angiosperm polycomb repressive complex 2 subunit
548 VERNALIZATION 2, *Nat. Commun.* (2018). doi:10.1038/s41467-018-07875-7.
- 549 [39] D.A. Weits, N.C.W. Kunkowska, Alicja B. Kamps, K. Portz, Z. Packbier, Niko K. Nemeč-Venza, J.U.
550 Gaillochet, Christophe Lohmann, O. Pedersen, F. van Dongen, Joost T. Licausi, An apical hypoxic
551 niche sets the pace over shoot meristem activity, *Nature*. (n.d.).
- 552 [40] R.R. Schmidt, M. Fulda, M. V Paul, M. Anders, F. Plum, D.A. Weits, M. Kosmacz, T.R. Larson, I.A.
553 Graham, G.T.S. Beemster, F. Licausi, P. Geigenberger, J.H. Schippers, J.T. van Dongen, Low-oxygen
554 response is triggered by an ATP-dependent shift in oleoyl-CoA in Arabidopsis,
555 *Proc. Natl. Acad. Sci.* 115 (2018) E12101 LP-E12110. doi:10.1073/pnas.1809429115.
- 556 [41] F. Wang, Z.H. Chen, S. Shabala, Hypoxia Sensing in Plants: On a Quest for Ion Channels as Putative
557 Oxygen Sensors, *Plant Cell Physiol.* (2017). doi:10.1093/pcp/pcx079.
- 558 [42] S. Iacopino, S. Jurinovich, L. Cupellini, L. Piccinini, F. Cardarelli, P. Perata, B. Mennucci, B. Giuntoli, F.
559 Licausi, A synthetic oxygen sensor for plants based on animal hypoxia signalling, *Plant Physiol.*
560 (2019). doi:10.1104/pp.18.01003.
- 561 [43] J.M. Gardner, S.L. Jaspersen, Manipulating the yeast genome: Deletion, mutation, and tagging by
562 PCR, *Methods Mol. Biol.* 1205 (2014) 45–78. doi:10.1007/978-1-4939-1363-3_5.
- 563 [44] A. Wach, A. Brachat, R. Pöhlmann, P. Philippsen, New heterologous modules for classical or PCR-
564 based gene disruptions in *Saccharomyces cerevisiae*, *Yeast.* 10 (1994) 1793–1808.

565 doi:10.1002/yea.320101310.

566 [45] R.D. Gietz, R.H. Schiestl, Frozen competent yeast cells that can be transformed with high efficiency
567 using the LiAc/SS carrier DNA/PEG method, *Nat. Protoc.* 2 (2007) 1–4. doi:10.1038/nprot.2007.17.

568 [46] T. von der Haar, Optimized protein extraction for quantitative proteomics of yeasts, *PLoS One.* 2
569 (2007). doi:10.1371/journal.pone.0001078.

570 [47] M.E. Schmitt, T.A. Brown, B.L. Trumpower, A rapid and simple method for preparation of RNA from
571 *Saccharomyces cerevisiae*, *Nucleic Acids Res.* (1990). doi:10.1093/nar/18.10.3091.

572 [48] K.J. Livak, T.D. Schmittgen, Analysis of Relative Gene Expression Data Using Real-Time Quantitative
573 PCR and the $2^{-\Delta\Delta CT}$ Method, *Methods.* 25 (2001) 402–408. doi:10.1006/meth.2001.1262.

574